

RESEARCH

Open Access



Photoplethysmography parameters in monitoring nociception during general anesthesia

Hua Li^{1†}, Yingying Tang^{2†}, Xiaoping Chen², Mengge Zhang³, Feng Jiang³, Fangfang Zhu², Linghua Xie², Hui Wu², Qi Xu², Qing Chen², Shulan Xie², Ange Dai² and Xinzhong Chen^{2*}

Abstract

Background Validated monitoring methods for evaluating the balance of nociception and anti-nociception (BNAN) are needed in general anesthesia. This study assessed six photoplethysmography (PPG) parameters, computed from finger photoplethysmographic waveforms in patients undergoing gynecological surgery under general anesthesia.

Methods A total of 20 participants were included, each undergoing general anesthesia with propofol and remifentanyl. The same concentration of remifentanyl was maintained throughout the experiment, four different intensities of electrical stimulation were administered, and the patient's fingertip PPG was meticulously recorded. PPG data were preprocessed to extract six PPG morphological parameters, and photoplethysmographic amplitude (PPGA), pulse beat interval (PBI), and surgical pleth index (SPI). Receiver operating characteristic (ROC) curves and the Area Under the Curve (AUC) were constructed and calculated to accurately measure its ability to reflect the nociceptive stimulus state. The consistency of different phase parameters at different stimulus intensities was evaluated by calculating the prediction probabilities. All results were compared with those obtained using SPI, PPGA, and PBI.

Results After stimulation, all parameters and SPI showed significant changes compared with those before stimulation ($p=0.000$). The catacrotic phase parameters (AC and MHC) showed higher discrimination in adequate analgesia and congruence with electrical stimulation intensity than the overall phase parameters, PPGA, and anacrotic phase parameters (AC: AUC = 0.851, Pk = 0.800; MHC: AUC = 0.837, Pk = 0.792).

Conclusions In this study, six PPG morphological parameters were proposed and observed for the first time to effectively distinguish the occurrence of nociception. Compared with the overall phase parameters, PPGA, and anacrotic phase parameters, catacrotic phase parameters were more capable of characterizing noxious stimuli and more consistent with changes in electrical stimulation intensity.

Trial registration ChiCTR2200062228; Registered at <http://clinicaltrials.gov> on July 30, 2022.

Keywords Photoplethysmography, General anesthesia, The balance of nociception and anti-nociception

[†]Hua Li and Yingying Tang contributed equally to this work.

*Correspondence:
Xinzhong Chen
chenxinz@zju.edu.cn

¹Department of Anesthesia, The third people's hospital of Hefei. Hefei Third Clinical College, Anhui Medical University, Hefei, China

²Department of Anesthesia, Women's Hospital, Zhejiang University School of Medicine, Hangzhou, China

³College of Biomedical Engineering and Instrument Science, Zhejiang University, Hangzhou, China



Background

Under general anesthesia (GA), pain is redefined as nociception, the physiological response to noxious stimuli, because patients are unconscious and unable to perceive pain [1, 2]. The balance of nociception and anti-nociception (BNAN) reflects the interaction between noxious input and the body's counteracting mechanisms, making its monitoring essential for optimizing analgesia.

Effective BNAN monitoring is crucial for ensuring optimal pain management while minimizing the risks associated with inadequate analgesia or opioid overuse. Inadequate intraoperative analgesics might cause excessive postoperative pain, while inadequate treatment might also promote inflammation, and hormonal and immune imbalance [3–6]. On the other hand, opioid overdose may cause postoperative pain hypersensitivity and worsen opioid-induced respiratory depression (OIRD) [7]. Current BNAN monitoring methods include motor reflex monitoring, central nervous system (CNS) monitoring, and autonomic nervous system (ANS) monitoring [8]. Among these, ANS-based monitoring has gained attention owing to its noninvasive nature and real-time feedback potential. However, current physiological markers, such as skin conductance [9] and pupil diameter [10], often lack the accuracy and consistency required for effective clinical applications.

In recent years, the potential of photoplethysmography (PPG) in measuring BNAN has sparked tremendous interest. PPG parameters, such as photoplethysmographic amplitude (PPGA), pulse beat interval (PBI), and surgical pleth index (SPI) calculated from PPGA and heart beat interval (HBI), primarily reflect changes in autonomic nervous system (ANS) activity. These changes may indirectly relate to nociceptive processes but do not directly characterize nociception itself [11–14] and are inadequately sensitive to varying intensities of noxious stimulation. This study aims to address these issues by introducing novel PPG waveform parameters and evaluating their reliability in detecting nociceptive stimuli and assessing analgesia adequacy.

Standardized electrical stimulation protocols are commonly employed to mimic clinical nociceptive events, such as surgical incisions [15], under controlled conditions. These protocols elicit measurable ANS responses and enable reproducible assessments of BNAN by distinguishing between adequate and inadequate analgesia states. Through controlled electrical stimuli, PPG-derived parameters can be systematically evaluated to establish their reliability in detecting nociceptive responses and contribute to more precise analgesic interventions.

A single PPG waveform consisted of an anacrotic phase and a catacrotic phase (Fig. 1). In this study, we identified and characterized six morphometric parameters of the PPG waveform, including the area under the curve of

anacrotic phase (AA) and the mean height of anacrotic phase in terms of area (MHA), the area under curve of catacrotic phase (AC) and the mean height of catacrotic phase in terms of area (MHC), and area under curve of a total period (AT) and the mean height of a wave in terms of area (MH). Our preliminary hypothesis was that these parameters might be utilized as tools to monitor BNAN under general anesthesia, and these results will be compared with those of PPGA, PBI, and SPI.

Methods

Ethics

The study was approved by the Ethical Committee of Women's Hospital, Zhejiang University School of Medicine (Hangzhou, China) (No. IRB-20220149-R) on April 21, 2022, and registered at Chinese Clinical Trials.gov (No. ChiCTR2200062228). The study was conducted from August 2022 to August 2023. All participants were informed of the purpose of the study and signed consent forms.

Study population

Twenty patients aged between 18 and 60 years, American Society of Anesthesiologists (ASA) I or II, with a body mass index (BMI) of 18–30 kg/m² scheduled for elective gynecological surgery participated in the study. Exclusion criteria were recently used sedatives, antidepressants, or other agents affecting PPG monitoring; abnormal neurological, cardiac, pulmonary, hepatic, or renal function; cardiovascular diseases such as hypertension; or receiving treatments that affect the cardiovascular system. Patients with diabetes mellitus, a history of alcoholism and/or substance misuse, or anemia (hemoglobin < 110 g/L) also fell outside the criteria.

Study protocol

Venous access was established after patients entered the operating room, connected to the GE Healthcare CARESCAPE B650 anesthesia monitor, which integrated electrocardiogram (ECG), noninvasive blood pressure (NIBP), SPI, response entropy (RE) state entropy (SE), and SpO₂. The entropy sensor (Entropy EasyFit Sensor M1174413) was fixed after thoroughly cleaning the patient's forehead according to the manufacturer's recommendations. Finger PPG data were also obtained using the same right index finger used for SpO₂. The Digitimer Train/Delay Generator Model DG2A was utilized as the electrical stimulator, which could generate the low power current at the specified intensity and frequency as well as the duration.

The protocol of the study was demonstrated in Fig. 2. Target-controlled infusion (TCI) of propofol and remifentanyl reached a concentration of 4 µg/ml and 4ng/ml in the effector chamber respectively, following the

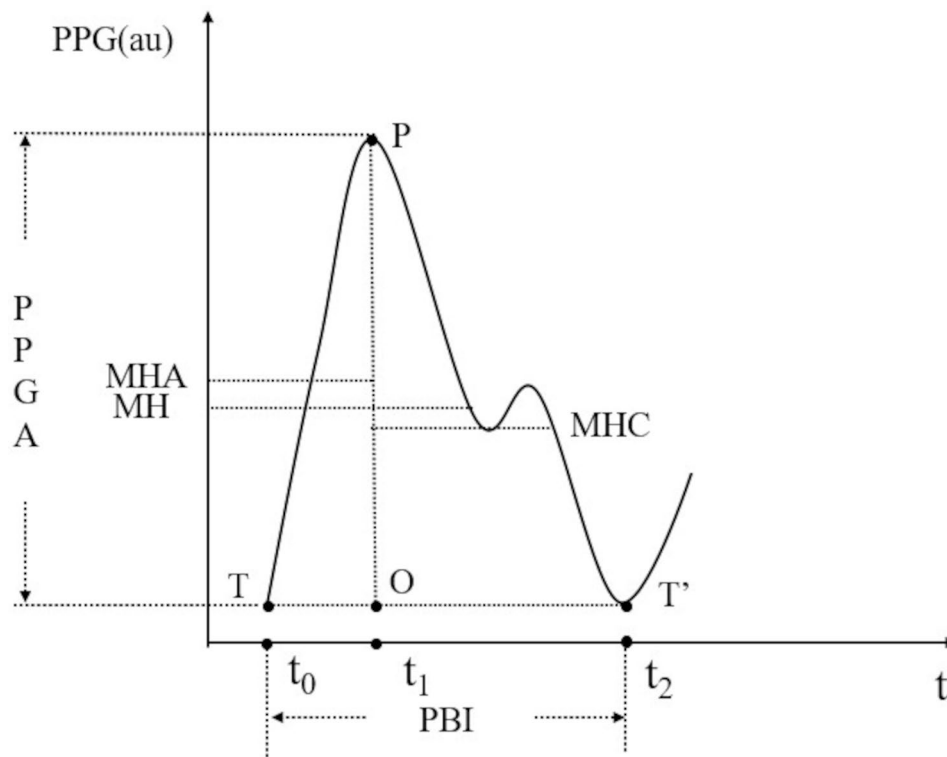


Fig. 1 Waveform characteristics of a PPG and parameter diagram

T: the trough of a PPG. P: the peak of a PPG. T': the next trough. O: the vertical projection of point P on the TT line
 TP: the anacrotic phase. T': the catacrotic phase. TT': the overall phase. t_0-t_1 : the interval of anacrotic phase. t_1-t_2 : the interval of the catacrotic phase. t_0-t_2 : the interval of the overall phase
 PPGA: the amplitude of OP; PBI: the interval of TT'; SPI was computed as a combination of the normalized PPGA and heart beat interval (HBI), $SPI = 100 - (0.7 * PPGA_{norm} + HBI_{norm})$

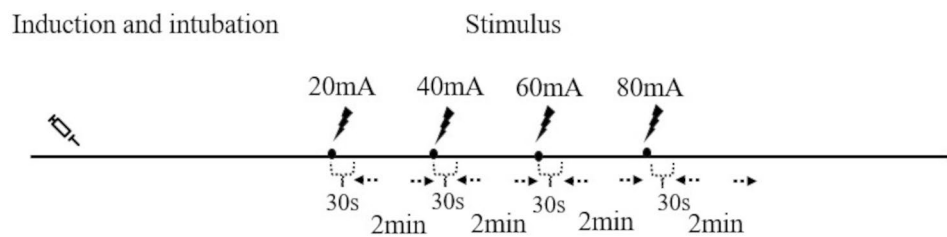


Fig. 2 Study protocol

pharmacokinetic model of the previous researches [16, 17]. Meanwhile, the concentration of propofol was adjusted under the SE, keeping within the 40–60 range, and 0.6 mg/kg rocurium bromide was injected. Following this, intubation and controlled ventilation were initiated. The left ulnar nerve was continuously stimulated using the electrical stimulator above at the gradient current intensities of 20, 40, 60, and 80 mA respectively, and a stationary frequency of 50 Hz, duration of 30s. Based on Rantanen’s finding [15], tetanic stimulation (50 mA) mimics the autonomic response of surgical stimulation. Stimulation at 20 or 40 mA was categorized as mild nociceptive stimulation, indicating adequate analgesia, while 60 or 80 mA was classified as strong nociceptive

stimulation, reflecting insufficient analgesia. By selecting electrical stimulation intensities ranging from 20 to 80 mA, this study simulates mild to severe clinical pain conditions to validate the reliability of new PPG parameters in distinguishing analgesia adequacy.

Four stimuli were performed every 2 min with an operated time manually recorded on the monitor as well. Before and after each electrical stimulation, the SPI was collected and PPG was recorded continuously for at least 120s.

Data processing

The PPG signals were preprocessed offline after exporting them from the GE B650 device. Then PPG

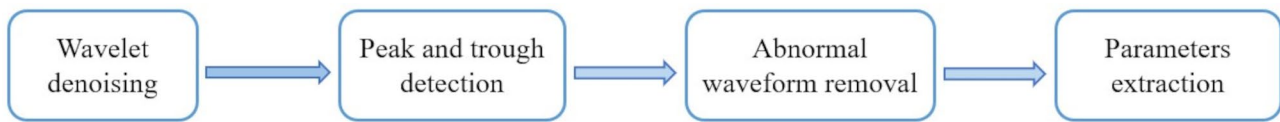


Fig. 3 The flowchart of data processing

Table 1 Definition and illustration of parameters

parameters	definition	graphical interpretation
AA	the area under curve of the anacrotic phase	the area of the OPT curve
AC	the area under curve of the catacrotic phase	the area of the OPT' curve
AT	the area under curve of a total period	the area of the TPT' curve
MHA	the mean height of the anacrotic phase in terms of area	$MHA = \frac{1}{t_1-t_0} \int_{t_0}^{t_1} p(t) dt$
MHC	the mean height of the catacrotic phase in terms of area	$MHC = \frac{1}{t_2-t_1} \int_{t_1}^{t_2} p(t) dt$
MH	the mean height of a wave in terms of area	$MH = \frac{1}{t_2-t_0} \int_{t_0}^{t_2} p(t) dt$
PBI	pulse beat interval	the time interval between adjacent troughs, T-T'
PPGA	the photoplethysmography amplitude	The height of line OP

preprocessing was conducted, including wavelet denoising, peak and trough detection, and abnormal waveform detection and removal, as the flowchart presented in Fig. 3. Then 8 types of morphologic parameters were extracted and derived from PPG pulses, including PPGA, PBI, and 6 morphometric parameters, whose definitions can be found in Table 1. Two intervals, -60s to -30s and 0 to +30s, were selected to represent PPG states before and after electrical stimulation onset, whereas the plus sign before the digit indicates a post-stimulus interval and a minus sign indicates a pre-stimulus interval. The value before stimulation was calculated as the average value within the pre-stimulus interval, while the value after stimulation was calculated as the minimum value of the post-stimulus interval.

To eliminate the influence of outliers, 8 raw parameters above were processed further as follows. First, both the pre-stimulus and post-stimulus parameters were calculated based on PPG waveforms. Subsequently, a mean filter with a window of 10s was applied to them, with the window shifted forward by 1s each time. Finally, raw parameters were obtained by calculating the mean of their corresponding values in the first step. To eliminate individual differences and improve the parameters' responsiveness to noxious stimuli, an extra normalization was carried out to remap the original values to the interval of [0, 1], as shown in Eq. 1.

$$Y_i = \frac{X_i - \bar{X}}{\mu} \quad (1)$$

where X_i represents the parameter input, \bar{X} represents the mean of input X , μ stands for the standard deviation (SD) of X , and Y_i for the output after the normalization.

This normalization ensures that all parameter values are expressed on a standardized scale, facilitating more accurate comparisons and reducing potential biases caused by individual differences.

Based on the distinction of data utilized to calculate the value of a parameter, except the common parameters in the clinic PBI and PPGA, the remaining 6 morphologic parameters in Table 1 could be further divided into three groups: the anacrotic phase group (AA and MHA), the catacrotic phase group (AC and MHC) and the overall phase (AT and MH).

Statistical analysis

The normal distribution measures were expressed as the mean \pm SD, whereas non-normally distributed measures were expressed as the median (quartiles). The difference between post- and pre- in AA, AC, AT, MHA, MHC, MH, PPGA, PBI, and SPI at each stimulation intensity (20 mA, 40 mA, 60 mA, and 80 mA) were calculated, with the variation expressed as Δ values. A linear mixed-effects model with an unstructured covariance matrix was used to analyze these changes, treating them as dependent variables and stimulation intensity as a four-level categorical independent variable. The Paired rank-sum test was utilized for intra-group comparison, with Bonferroni adjustment applied to control for multiple comparisons. It was deemed statistically significant if the value of p is less than 0.05.

The receiver operating characteristic (ROC) curves and the area under the curve (AUC) were employed to assess the discriminatory capability of PPG parameters between low-intensity stimulation (20–40 mA) and high-intensity stimulation (60–80 mA). The Youden Index (YI), the sum of sensitivity and specificity minus 1, is a common diagnostic validity index. The index ranges from -1 to 1, with

Table 2 The characteristics of participants

	Range	Value
Age(yr)	27–53	39±8
Height(cm)	150–170	161±6
Weight(kg)	46–55	55±5

the max value indicating relatively highest effectiveness [18]. To evaluate the consistency of characteristic parameters and SPI with varying electrical stimulation intensities, prediction probabilities (Pk) were calculated using the PKMACRO spreadsheets as described by Smith et al. [19].

SPSS (IBM SPSS Statistics 26.0.0) was employed to perform the above analyses and the graphs were designed based on Origin (Version 2021. OriginLab Corporation, Northampton, MA, USA).

Results

The characteristics of participants

The sample size was determined to be 20 based on previous studies [20, 21]. We recruited 20 patients for this study, and all the analyses were carried out based on the 20 patients. The characteristics of them are summarized in Table 2.

The ability to distinguish the occurrence of stimuli

For the two intervals representing the pre-stimulus and post-stimulus, the 8 parameters defined in Table 1 together with the SPI were calculated respectively, as contrasted in Table 3; Fig. 4. During stimulation, SPI increased from 22.000 to 29.000, while the remaining 8 parameters showed a downward trend with statistical significance ($p=0.000$). In summary, all 8 parameters and SPI responded positively to electrical stimulation.

Effects of different intensities of stimulation on parameters

In addition, the role of current intensities in parameters has also been studied in this research. The parameters, including ΔAA , ΔAC , ΔPBI and ΔSPI , were significantly influenced by stimulation intensity (ΔAA , $p=0.015$; ΔAC , $p=0.042$; ΔPBI , $p=0.033$; ΔSPI , $p=0.028$). When

a stimulus was performed at a certain current intensity between 20, 40, 60, and 80 mA, the above parameters and SPI were calculated and compared, as shown in Fig. 5. There were statistical differences for PPGA ($p=0.029$), AT ($p=0.029$), MHA ($p=0.042$), and MHC ($p=0.029$) when comparing 20 mA and 40 mA. Significant differences were observed for all characteristic parameters except MHA when comparing results under 20 mA stimulation intensity with 60 mA ($p=1.000$) and 80 mA ($p=1.000$). When comparing the results between 40 mA and 60 mA, only PBI ($p=0.029$) and SPI ($p=0.005$) showed significant differences. When 40 mA was compared with 80 mA, all parameters showed significant differences except PPGA ($p=0.224$), while AA ($p=0.020$), AC ($p=0.009$), AT ($p=0.020$), MHA ($p=0.006$), MHC ($p=0.009$), MH ($p=0.013$), PBI ($p=0.000$), SPI ($p=0.000$). There were no significant differences except MHA ($p=0.006$) when 60 mA stimulation intensity was compared with 80 mA.

The ability to differentiate between analgesia adequacy

To further assess the ability of the parameters to distinguish between adequate and inadequate analgesia, ROC curves were plotted for the parameters in Fig. 6, and the corresponding AUC and maximum Youden Index (YI) values were calculated. For the analysis, stimulation intensities of 20 mA and 40 mA were categorized as the adequate analgesia group, while 60 mA and 80 mA were classified as the inadequate analgesia group, as previously described. As shown in Table 4, in the AUC comparison, the AUC of PBI and SPI were equal and the largest (AUC=0.896), followed by AC (AUC=0.851), MHC (AUC=0.837), AT (AUC=0.829), MH and PPGA (AUC=0.784), AA (AUC=0.769) and MHA (AUC=0.722). Among the parameters in different phases, the AUC of catacrotic phase parameters (AC and MHC) was higher than that of overall phase parameters (AT and MH), PPGA, and anacrotic phase parameters (AA and MHA).

In the comparison of max YI, the values of PBI, SPI, and MHC were highest (YI=0.650), followed by AC (YI=0.575), AT (YI=0.525), AA (YI=0.500), MH and

Table 3 Comparison of parameters of the pre-stimulus and post-stimulus

parameters/group	pre-stimulus	post-stimulus	post-pre(p)
AA	-0.002(-0.015, 0.006)	-0.568(-1.148, -0.090)	0.000*
AC	-0.005(-0.020, 0.006)	-0.511(-0.930, -0.109)	0.000*
AT	-0.004(-0.018, 0.006)	-0.598(-1.213, -0.111)	0.000*
MHA	0.000(-0.014, 0.008)	-0.271(-0.574, 0.020)	0.000*
MHC	0.893(0.617, 1.315)	0.408(-0.194, 0.935)	0.000*
MH	-0.004(-0.014, 0.006)	-0.398(-0.815, -0.062)	0.000*
PBI	-0.005(-0.015, 0.009)	-0.101(-0.214, 0.067)	0.000*
PPGA	-0.003(-0.017, 0.009)	-0.916(-1.954, -0.142)	0.000*
SPI	22.000(18.000, 30.750)	29.000(21.250, 39.500)	0.000*

Values are displayed as median(quartiles). * $p < 0.05$

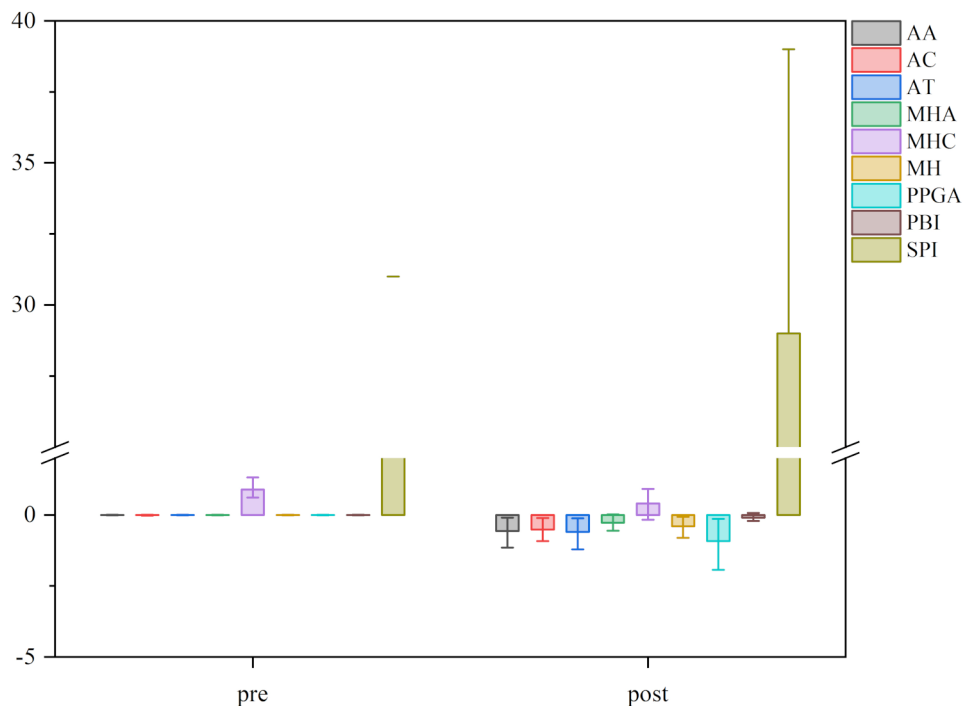


Fig. 4 The pre-stimulus and post-stimulus of parameters and SPI

The box plot shows the median, with I-shaped lines as error bars for the first and third quartiles. "pre-" indicates the pre-stimulation state, and "post-" the post-stimulation state

PPGA (YI=0.475), MHA (YI=0.400). Among the parameters in different phases, the maximum YI of catacrotic phase parameters was higher than the overall phase parameters, PPGA, and anacrotic phase parameters, while these findings were consistent with the AUC.

The curve highlights sensitivity and specificity across various thresholds, with the AUC values representing the overall discriminative ability.

The consistency with electrical stimulation intensity

To compare the consistency of characteristic parameters and SPI with electrical stimulation intensity, prediction probabilities (Pk) were calculated. As shown in Table 5, SPI performed best (Pk=0.853), followed by PBI (Pk=0.809), AC (Pk=0.800), MHC (Pk=0.792), AT (Pk=0.785), PPGA (Pk=0.749), MH (Pk=0.745), AA (Pk=0.743), MHA (Pk=0.690). Among the parameters in different phases, the Pk of catacrotic phase parameters was higher than the overall phase parameters, PPGA, and anacrotic phase parameters, while these results were consistent with the AUC.

Discussion

In our study, it was suggested that AA, AC, AT, MHA, MHC, and MH could distinguish the occurrence of electrical stimulation. Notably, the catacrotic phase parameters (AC and MHC) outperformed the overall phase parameters (AT and MH), PPGA, and the anacrotic

phase parameters (AA and MHA) in distinguishing the adequacy of analgesia and varied degrees of tetanic stimulation.

The correlation between the PPG and BNAN

In recent years, a variety of monitoring indicators have been developed to evaluate and control the BNAN in GA. Traditional indexes encompass heart rate (HR) and blood pressure (BP), autonomic response-based metrics like pupillary diameter (PD) [10, 22], and skin conductance (SC) [9, 23–25], indicators developed based on PPG and EEG like the SPI [14, 26], analgesia nociception index (ANI) [27–30] and multi-parametric index nociception level index (NOL) [31–34]. Although these indicators monitor the BNAN to some extent, they remain distant from an ideal and precise index for analgesia depth monitoring [32, 33, 35, 36]. As the correlation between the PPG and BNAN has been extensively analyzed, PPGA is thought to be associated with nociception in GA [37], and this PPGA can be augmented by the onset of noxious stimuli [38]. In addition, PBI was identified as associated with nociception during general anesthesia and declined with the occurrence of noxious stimulation [39]. Our study also found that the PPGA, PBI, and SPI were also able to distinguish between sufficient analgesia and different degrees of tetanic stimulus, which is in line with the findings of earlier research [14, 37, 40]. Among these parameters, PBI prevailed over the

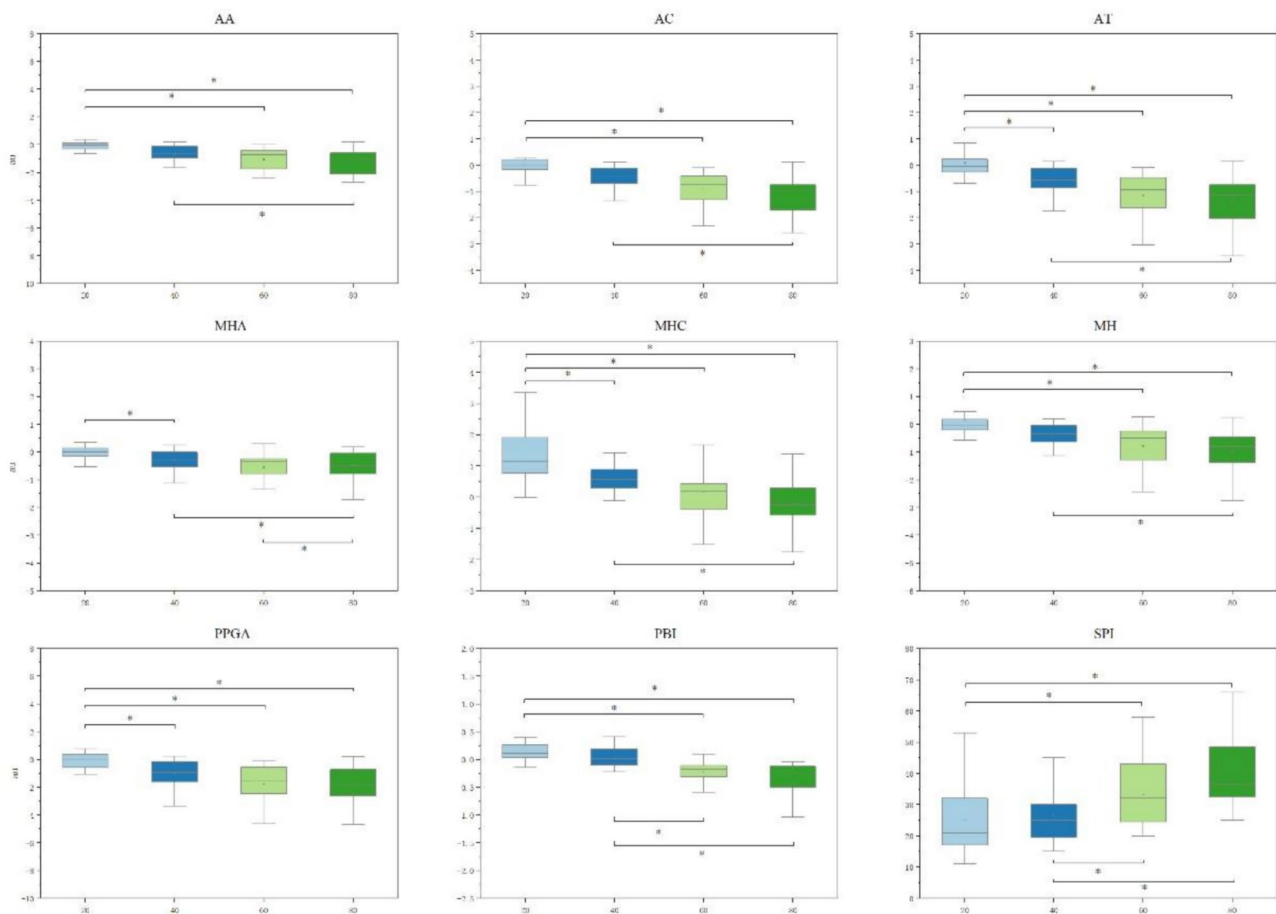


Fig. 5 Intergroup comparison of parameters. Boxes represent IQR, where the line with the point represents the median. Whiskers at the top and bottom of the box represent the highest and lowest values, * means $p < 0.05$

PPGA in distinguishing between sufficient analgesia and different degrees of stimulation, though the performance of all parameters lagged behind the SPI.

The possible mechanism of PPG and BNAN

As we know, the anacrotic phase of PPG represents rapid ventricular ejection while the catacrotic phase reflects a reduced ejection phase and diastole. When patients experience nociception, the surgical stress response is typically characterized by increased production and release of pituitary hormones and activation of the sympathetic nervous system (SNS) [41]. The activation of the ANS by the hypothalamus further enhances the release of catecholamines from the adrenal medulla, and the release of norepinephrine from presynaptic nerve endings [37, 42]. Norepinephrine then interacts with α -adrenergic receptors on finger blood vessels, resulting in a vasoconstriction effect and an increase in the magnitude of vasoconstriction during the catacrotic phase of PPG. This may be one possible explanation for the higher correlation between catacrotic phase parameters and BNAN. It is worth noting that the better performance of catacrotic

phase parameters (AA and MHA) in monitoring BNAN is corroborated by our previous study [21], which revealed that catacrotic phase-characterizing parameters, including diastolic interval (DI), diastolic slope (DS) and the nearest trough of minimum slope during catacrotic phase (DTI), could provide promising potential to qualify BNAN.

PPG parameters in adequate analgesia or hypo analgesia

Studies by Rantanen [15] have concluded that tetanic electrical stimulation (30 s, 50 mA, and 50 Hz) is necessary to elicit the identical level of ANS response as clinical surgical stimulation (such as incisions). Thus, we characterize stimulation at 20 or 40 mA to represent a lack of perceptible or a lesser degree of nociceptive stimulation, indicating adequate analgesia. Conversely, stimulation at 60 or 80 mA was designated as the capacity to perceive nociceptive stimulation or a higher degree of nociceptive stimulation, indicating insufficient analgesia. In our study, a preliminary observation was made about the ability of PPG parameters to distinguish between

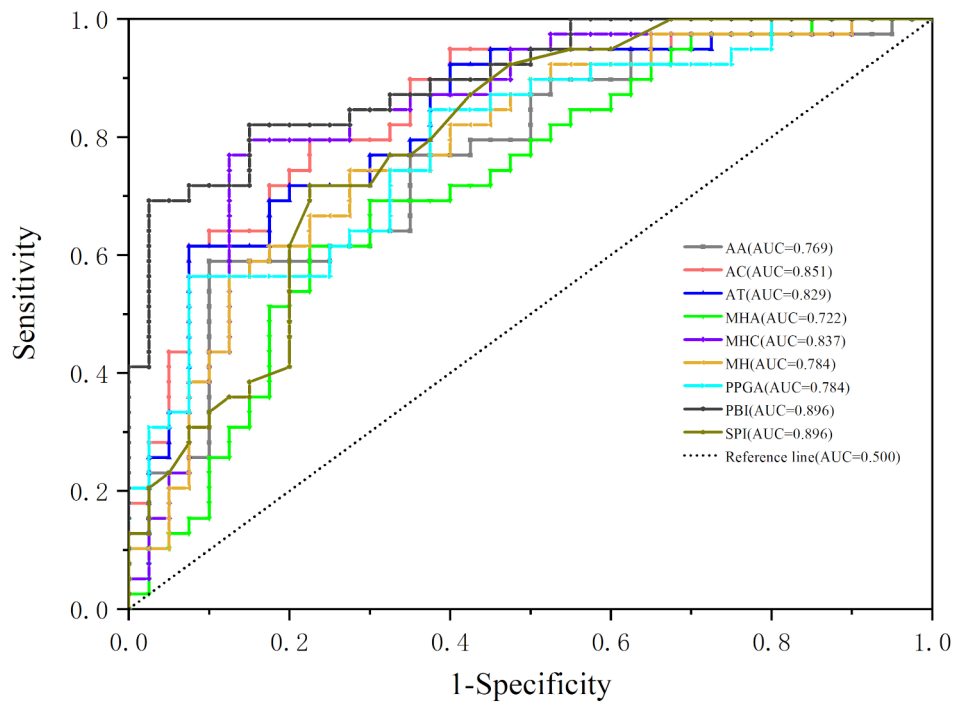


Fig. 6 The ROC of parameters

Table 4 The AUC and YI of parameters

Parameters	AUC	The Max YI	Sensitivity	Specificity
AA	0.769	0.500	0.600	0.900
AC	0.851	0.575	0.800	0.775
AT	0.829	0.525	0.625	0.900
MHA	0.722	0.400	0.625	0.775
MHC	0.837	0.650	0.775	0.875
MH	0.784	0.475	0.750	0.725
PBI	0.896	0.650	0.675	0.975
PPGA	0.784	0.475	0.550	0.925
SPI	0.896	0.650	0.800	0.850

The sensitivity and specificity in the table were acquired when the YI got the max value

Table 5 The pk of parameters

Parameters	prediction probabilities (Pk)
AA	0.743(0.038)
AC	0.800(0.034)
AT	0.785(0.035)
MHA	0.690(0.045)
MHC	0.792(0.034)
MH	0.745(0.039)
PBI	0.809(0.028)
PPGA	0.749(0.039)
SPI	0.853(0.030)

Data are expressed as the Pk values with standard error

adequate pain relief and overmedication, but a lack of reliability on detecting hypo analgesia.

Possible influencing factors and solutions

As various factors such as drugs and the environment may influence PPG signals, this study aimed to optimize the PPG signal through the preprocessing and normalization process to extract clean and undistorted signals, remove respiratory interference and individual differences, and eliminate potential interference from other factors to the greatest extent. To ensure sedation depth was maintained within the appropriate range, SE was maintained between 40 and 60 throughout the study, ruling out any influence of sedative drugs.

Limitations and prospects

While there are several strengths to our research, it does have some limitations. For example, we focused only on the parameter response to tetanic stimulation at one remifentanyl concentration, other concentrations and types of analgesics needed to be further investigated. In addition, our study participants were all adult females. Given the gender disparities in analgesia, the study should have been expanded to include both genders and a wider age range [43].

Conclusions

In this study, six morphological parameters of PPG were proposed and observed for the first time to distinguish the occurrence of noxious stimulation effectively. Compared with overall phase parameters, PPGA, and anacrotic phase parameters, catacrotic phase parameters were more capable of characterizing noxious stimuli and more consistent with changes in electrical stimulation intensity.

Abbreviations

GA	General anesthesia
BANA	Balance of nociception-anti-nociception
OIRD	Opioid-induced respiratory depression
CNS	Central nervous system
ANS	Autonomic nervous system
PPG	Photoplethysmography
PPGA	Photoplethysmographic amplitude
PBI	Pulse beat interval
SPI	Surgical pleth index
HBI	Heart beat interval
AA	Area under curve of anacrotic phase
MHA	Mean height of anacrotic phase in terms of area
AC	Area under curve of catacrotic phase
MHC	Mean height of catacrotic phase in terms of area
AT	Area under curve of a total period
MH	Mean height of a wave in terms of area
ASA	American Society of Anesthesiologists
BMI	Body mass index
ECG	Electrocardiogram
NIIBP	Noninvasive blood pressure
RE	Response entropy
SE	State entropy
TCI	Target-controlled infusion
SD	Standard deviation
ROC	Receiver operating characteristic
AUC	Area under the curve
YI	Youden Index
Pk	Prediction probabilities
HR	Heart rate
BP	Blood pressure
PD	Pupillary diameter
ANI	Analgesia nociception index
NOL	Nociception level index

Acknowledgements

This study was supported by the National Nature Science Foundation of China (NSFC) (Grant number: 81870868).

Author contributions

Conceptualization: Hua Li, Xiaoping Chen, Mengge Zhang, Yingying Tang. Writing – original draft and Validation: Hua Li, Xiaoping Chen, Mengge Zhang, Xinzhong Chen; Resources and Project administration: Hua Li, Xiaoping Chen, Mengge Zhang, Fangfang Zhu, Ange Dai; Supervised the data analysis and Writing – review & editing: Yingying Tang, Feng Jiang, Qi Xu; Visualization and Software: Feng Jiang, Qi Xu; Supervision and Resources: Yingying Tang, Xiaoping Chen, Xinzhong Chen; Methodology and Data curation: Xiaoping Chen, Hui Wu, Linghua Xie, Qing Chen, Shulan Xie, Xinzhong Chen; Funding acquisition: Xinzhong Chen.

Funding

Xinzhong Chen.

Data availability

The datasets used and/or analysed during the current study are available from the corresponding author on reasonable request.

Declarations

Ethics approval and consent to participate

The study was approved by the Ethical Committee of Women's Hospital, Zhejiang University School of Medicine (Hangzhou, China) (No. IRB-20220149-R) on April 21, 2022, and registered at Chinese Clinical Trials.gov (No. ChiCTR2200062228). The study was conducted from August 2022 to August 2023. All participants were informed of the purpose of the study and signed consent forms.

Consent for publication

Not applicable.

Competing interests

The authors declare no competing interests.

Received: 3 October 2024 / Accepted: 28 January 2025

Published online: 17 February 2025

References

1. Rantanen M, Yli-Hankala A, van Gils M, Yppärilä-Wolters H, Takala P, Huiku M, Kymäläinen M, Seitsonen E, Korhonen I. Novel multiparameter approach for measurement of nociception at skin incision during general anaesthesia. *Br J Anaesth.* 2006;96(3):367–76.
2. Raja SN, Carr DB, Cohen M, Finnerup NB, Flor H, Gibson S, Keefe FJ, Mogil JS, Ringkamp M, Sluka KA, et al. The revised International Association for the study of Pain definition of pain: concepts, challenges, and compromises. *Pain.* 2020;161(9):1976–82.
3. Vallejo R, Hord ED, Barna SA, Santiago-Palma J, Ahmed S. Perioperative immunosuppression in cancer patients. *J Environ Pathol Toxicol Oncol.* 2003;22(2):139–46.
4. Tsuchiya Y, Sawada S, Yoshioka I, Ohashi Y, Matsuo M, Harimaya Y, Tsukada K, Saiki I. Increased surgical stress promotes tumor metastasis. *Surgery.* 2003;133(5):547–55.
5. Crozier TA, Müller JE, Quittkat D, Sydow M, Wuttke W, Kettler D. Effect of anaesthesia on the cytokine responses to abdominal surgery. *Br J Anaesth.* 1994;72(3):280–5.
6. Schrickler T, Carli F, Schreiber M, Wachter U, Geisser W, Lattermann R, Georgieff M. Propofol/sufentanil anesthesia suppresses the metabolic and endocrine response during, not after, lower abdominal surgery. *Anesth Analg.* 2000;90(2):450–5.
7. Baldo BA, Rose MA. Mechanisms of opioid-induced respiratory depression. *Arch Toxicol.* 2022;96(8):2247–60.
8. Laferrière-Langlois P, Morisson L, Jeffries S, Duclos C, Espitalier F, Richebé P. Depth of Anesthesia and Nociception Monitoring: current state and vision for 2050. *Anesth Analg.* 2024;138(2):295–307.
9. Ledowski T, Ang B, Schmarbeck T, Rhodes J. Monitoring of sympathetic tone to assess postoperative pain: skin conductance vs surgical stress index. *Anaesthesia.* 2009;64(7):727–31.
10. Barvais L, Engelman E, Eba JM, Coussaert E, Cantraine F, Kenny GN. Effect site concentrations of remifentanyl and pupil response to noxious stimulation. *Br J Anaesth.* 2003;91(3):347–52.
11. Dorlas JC, Nijboer JA. Photo-electric plethysmography as a monitoring device in anaesthesia. Application and interpretation. *Br J Anaesth.* 1985;57(5):524–30.
12. Kallio H, Lindberg LI, Majander AS, Uutela KH, Niskanen ML, Paloheimo MPJ. Measurement of surgical stress in anaesthetized children. *Br J Anaesth.* 2008;101(3):383–9.
13. Feng Y, Chen X, Wang X, Fu F, Chen H, Bein B. Area difference ratio for assessing nociceptive balance during laryngoscopy and intubation under intravenous anaesthesia: preliminary investigation of a novel photoplethysmographic variable. *Eur J Anaesthesiol.* 2015;32(1):58–9.
14. Huiku M, Uutela K, van Gils M, Korhonen I, Kymäläinen M, Meriläinen P, Paloheimo M, Rantanen M, Takala P, Viertiö-Oja H, et al. Assessment of surgical stress during general anaesthesia. *Br J Anaesth.* 2007;98(4):447–55.
15. Rantanen M, Yppärilä-Wolters H, van Gils M, Yli-Hankala A, Huiku M, Kymäläinen M, Korhonen I. Tetanic stimulus of ulnar nerve as a predictor of heart rate response to skin incision in propofol remifentanyl anaesthesia. *Br J Anaesth.* 2007;99(4):509–13.

16. Schnider TW, Minto CF, Gambus PL, Andresen C, Goodale DB, Shafer SL, Youngs EJ. The influence of method of administration and covariates on the pharmacokinetics of propofol in adult volunteers. *Anesthesiology*. 1998;88(5):1170–82.
17. Minto CF, Schnider TW, Shafer SL. Pharmacokinetics and pharmacodynamics of remifentanyl. II. Model application. *Anesthesiology*. 1997;86(1):24–33.
18. Schisterman EF, Perkins NJ, Liu A, Bondell H. Optimal cut-point and its corresponding Youden Index to discriminate individuals using pooled blood samples. *Epidemiology*. 2005;16(1):73–81.
19. Smith WD, Dutton RC, Smith NT. Measuring the performance of anesthetic depth indicators. *Anesthesiology*. 1996;84(1):38–51.
20. Wang X, Chen X, Ye S, Feng Y, Huang C, Hou L, Liu J, Chen H. Changes in the photoplethysmogram with tracheal intubation and remifentanyl concentration. *Anaesthesia*. 2012;67(12):1332–6.
21. Chen W, Feng Y, Chen X, Jiang F, Miao J, Chen S, Chen H. Effect of laryngeal mask airway insertion on parameters derived from Catacrotic Phase of Photoplethysmography under different concentrations of Remifentanyl. *IEEE J Transl Eng Health Med*. 2020;8:2700609.
22. Constant I, Nghe MC, Boudet L, Berniere J, Schraye S, Seeman R, Murat I. Reflex pupillary dilatation in response to skin incision and alfentanil in children anaesthetized with sevoflurane: a more sensitive measure of noxious stimulation than the commonly used variables. *Br J Anaesth*. 2006;96(5):614–9.
23. Storm H, Shafiei M, Myre K, Raeder J. Palmar skin conductance compared to a developed stress score and to noxious and awakening stimuli on patients in anaesthesia. *Acta Anaesthesiol Scand*. 2005;49(6):798–803.
24. Ledowski T, Pascoe E, Ang B, Schmarbeck T, Clarke MW, Fuller C, Kapoor V. Monitoring of intra-operative nociception: skin conductance and surgical stress index versus stress hormone plasma levels. *Anaesthesia*. 2010;65(10):1001–6.
25. Ledowski T, Bromilow J, Paech MJ, Storm H, Hacking R, Schug SA. Skin conductance monitoring compared with Bispectral Index to assess emergence from total i.v. anaesthesia using propofol and remifentanyl. *Br J Anaesth*. 2006;97(6):817–21.
26. Struys MMRF, Vanpeteghem C, Huiku M, Uutela K, Blyært NBK, Mortier EP. Changes in a surgical stress index in response to standardized pain stimuli during propofol-remifentanyl infusion. *Br J Anaesth*. 2007;99(3):359–67.
27. Nitzschke R, Fischer M, Funcke S. [Nociception monitoring: Method for intra-operative opioid control?]. *Anaesthesist*. 2021;70(9):735–52.
28. Jeanne M, Clément C, De Jonckheere J, Logier R, Tavernier B. Variations of the analgesia nociception index during general anaesthesia for laparoscopic abdominal surgery. *J Clin Monit Comput*. 2012;26(4):289–94.
29. Jeanne M, Delecroix M, De Jonckheere J, Keribedj A, Logier R, Tavernier B. Variations of the analgesia nociception index during propofol anaesthesia for total knee replacement. *Clin J Pain*. 2014;30(12):1084–8.
30. Daccache G, Caspersen E, Pegoix M, Monthé-Sagan K, Berger L, Fletcher D, Hanouz J-L. A targeted remifentanyl administration protocol based on the analgesia nociception index during vascular surgery. *Anaesth Crit Care Pain Med*. 2017;36(4):229–32.
31. Ben-Israel N, Kliger M, Zuckerman G, Katz Y, Edry R. Monitoring the nociception level: a multi-parameter approach. *J Clin Monit Comput*. 2013;27(6):659–68.
32. Edry R, Recea V, Dikust Y, Sessler DI. Preliminary intraoperative validation of the Nociception Level Index: a noninvasive nociception monitor. *Anesthesiology*. 2016;125(1):193–203.
33. Martini CH, Boon M, Broens SJL, Hekkelman EF, Oudhoff LA, Buddeke AW, Dahan A. Ability of the nociception level, a multiparameter composite of autonomic signals, to detect noxious stimuli during propofol-remifentanyl anaesthesia. *Anesthesiology*. 2015;123(3):524–34.
34. Meijer F, Honing M, Roor T, Toet S, Calis P, Olofsen E, Martini C, van Velzen M, Aarts L, Niesters M, et al. Reduced postoperative pain using Nociception Level-guided fentanyl dosing during sevoflurane anaesthesia: a randomised controlled trial. *Br J Anaesth*. 2020;125(6):1070–8.
35. Ledowski T. Monitoring nociception-getting 'there yet' might be easier with a road map. *Br J Anaesth*. 2017;119(4):716–7.
36. Constant I, Sabourdin N. Monitoring depth of anaesthesia: from consciousness to nociception. A window on subcortical brain activity. *Paediatr Anaesth*. 2015;25(1):73–82.
37. Paloheimo MPJ, Sahanne S, Uutela KH. Autonomic nervous system state: the effect of general anaesthesia and bilateral tonsillectomy after unilateral infiltration of lidocaine. *Br J Anaesth*. 2010;104(5):587–95.
38. Nijboer JA, Dorlas JC. Comparison of plethysmograms taken from finger and pinna during anaesthesia. *Br J Anaesth*. 1985;57(5):531–4.
39. Zhang L, Xu L, Zhu J, Gao Y, Luo Z, Wang H, Zhu Z, Yu Y, Shi H, Bao H. To clarify features of photoplethysmography in monitoring balanced anaesthesia, compared with cerebral State Index. *Med Sci Monit*. 2014;20:481–6.
40. Chen W, Jiang F, Chen X, Feng Y, Miao J, Jiao C, Chen S, Chen H. Photoplethysmography response to laryngeal mask airway insertion during Propofol-Remifentanyl Anaesthesia. *Annu Int Conf IEEE Eng Med Biol Soc*. 2019;2019:4664–8.
41. Desborough JP. The stress response to trauma and surgery. *Br J Anaesth*. 2000;85(1):109–17.
42. Hamill RW. RS: Peripheral autonomic nervous system. In: *Primer on the Autonomic Nervous System (2nd Edn)*. edn. Edited by Robertson D. London: Elsevier Academic 2004.
43. Greenspan JD, Craft RM, LeResche L, Arendt-Nielsen L, Berkley KJ, Fillingim RB, Gold MS, Holdcroft A, Lautenbacher S, Mayer EA, et al. Studying sex and gender differences in pain and analgesia: a consensus report. *Pain*. 2007;132(Suppl 1):S26–45.

Publisher's note

Springer Nature remains neutral with regard to jurisdictional claims in published maps and institutional affiliations.